IEEE Access
Multidisciplinary ⋮ Rapid Review ⋮ Open Access Journal

Received February 12, 2020, accepted March 7, 2020, date of publication March 16, 2020, date of current version March 31, 2020.

Digital Object Identifier 10.1109/ACCESS.2020.2980558

Accurate Position Estimation of Mobile Robot Based on Cyber-Physical-Social Systems (CPSS)

ZHILIANG ZHU, YINGLI WEN, ZHENGJIANG ZHANG, ZHENGBING YAN, SHIPEI HUANG, AND XIAOFENG XU

College of Electrical and Electronic Engineering, Wenzhou University, Wenzhou 325035, China

Corresponding author: Zhiliang Zhu (zlzhu@wzu.edu.cn)

This work was supported in part by the National Natural Science Foundation of China under Grant 61374167, and in part by the Natural Science Foundation of Zhejiang Province under Grant LZ16E050002 and Grant LGG18F010016.

ABSTRACT When planning the trajectory of a mobile robot, it is usually necessary to use sensors to collect a large amount of position information. Because traditional computing methods cannot effectively use huge data sources, an edge computing that implements edge intelligent services on the side of network edge near the data source is proposed, which speeds up the process of data processing. However, the data collected through sensors may contain gross errors. In general, the influence of gross errors on state estimation are rarely considered when using particle filter algorithms for state estimation. In fact, the measurements of dynamic systems are often affected by different types of gross errors in the actual application process. Therefore, it is a problem worth studying that how to detect and compensate for different types of gross errors. In this paper, an improved particle filter algorithm is proposed for the position estimation of mobile robot dynamic system. Firstly, the gross error identification method is used to identify the types of gross errors, and then the various gross errors are compensated. Finally, the particle filter algorithm based on the measurements compensation is obtained. Simulation experiments on the position estimation of mobile robots are carried out to verify the effectiveness of the proposed method in solving the measurements with gross errors. The precise position estimation of the mobile robot is achieved. Through the simulation experiments on the position estimation problem of mobile robots, it is verified that the proposed method is effective in solving the measurements with gross errors. And the accurate position estimation of the mobile robot is realized.

INDEX TERMS Particle filter, gross error, mobile robot, position estimation, CPSS, edge computing.

I. INTRODUCTION

With the deepening of networked applications, especially the rapid development of the Internet of Things, big data, cloud computing and edge computing, the integration of information and physical systems has become closer, and the network has become increasingly connected with human society [1]–[6]. Therefore, a social physical information system integrating people, machines, and information has been formed [7], [8]. In the tracking and positioning system of the mobile robot, sensors are used to collect position information [9], [10], and various algorithms are used to process the collected data. Among various algorithms, particle filter (PF) algorithm has become an important signal processing tool in solving nonlinear system tracking problems in recent years [11]. PF is a filter based on the Monte Carlo method for any form of state space model. It approximates the probability density function by finding a set of random samples propagating in the state space, and replaces the integral operation with the sample mean to obtain the minimum variance estimate of the system state [12]. It uses a series of finite particles to approximate its conditional probability density and allows these particles to self-propagate to simulate the evolution of conditional probability. When the number of particles tends to infinity, the approximate conditional probability density will also tend to the true conditional probability density [13]. The superiority of PF technology in nonlinear non-Gaussian systems makes it widely used in many fields. In the economy, it is applied to economic data forecasting. It is used for radar tracking of airborne objects, passive tracking of air-to-air and air-to-ground in the military. And it is used for video surveillance of cars or people in traffic control. In the era of

The associate editor coordinating the review of this manuscript and approving it for publication was Xiaokang Wang.

rapid development of big data and artificial intelligence, it is also used for the global localization of robots [14]. In view of the superiority of particle filter algorithm in real-time state estimation of nonlinear systems, this paper uses PF algorithm to estimate the position of mobile robots. In the process of estimating the state of the system by using PF, the collection of measurement data is an important basis for weight distribution. If the measured data is disrupted by sudden major disturbances—outliers, systematic biases and drifts—that is, affected by gross errors, the results of state estimation obtained using such measurements are inaccurate [15]. Therefore, when estimating the position of the mobile robot, the measurements containing the gross errors should be processed and then used for the update of the weights. There are also some scholars who propose various methods on how to detect and compensate for the measurement of gross errors. Vaghefi *et al.* used six data mining methods to identify outliers in flow experiments, and verified the effects of various methods for detecting outliers [16]. Based on the mathematical model of the sun's trajectory, Xie *et al.* used the traditional time-controlled algorithm to track the sun's trajectory, analyzed the main factors of the system tracking statics generated by the tracking device, and designed and designed a correctable tracking system for tracking biases. The method of static elimination is used to track the running track of the sun [17]. The method can improve the power generation efficiency of the photovoltaic system in the field of photovoltaic power generation. Wang *et al.* proposed a novel residual generator structure, which used fault detection mechanism and iterative estimation method to eliminate the tracking performance of sensor drift faults in unknown dynamic digital PID systems based on the estimated fault correction tracking error signal [18]. Zhang *et al.* proposed a new particle filter algorithm based on measurements detection for data correction and gross error detection of dynamic systems. When there are outliers in the obtained measurements, the method can effectively perform data correction and simultaneously detect whether the measurement data has gross error [19]. Maiz *et al.* proposed an outlier detection step to deal with the target tracking problem in the nonlinear state space model for the problem of outliers in nonlinear time series [20]. According to the above research literature, all the proposed methods propose corresponding solutions for a certain type of gross error, but there may be more than one gross error in the actual application system. Therefore, it is important for system state estimation by taking into account other different types of gross errors. With the rapid development of big data and artificial intelligence, mobile robots have achieved rapid development and wide application due to their large working space and strong adaptability [21]. And the efficient work of mobile robot is more dependent on the reliability of the self-localization algorithm [22]. For the position estimation of mobile robot, many scholars use different methods to improve the accuracy of positioning. Alatise *et al.* used Extended Kalman Filter (EKF) to fuse the data of the inertial sensors and the camera to estimate position of mobile robot for accurate positioning [23]. Dobrev *et al.* used extended Kalman filtering radar, ultrasonic and ranging sensors to achieve 3D position estimation of mobile robot for indoor applications [24]. However, extended Kalman filtering cannot be used for strong nonlinear systems, otherwise position estimation will not be accurate enough. Therefore, the particle filter algorithm can be used to process the position data when performing state estimation of nonlinear system. For example, Adrian *et al.* used wireless sensors and particle filter algorithms to improve the performance of position systems of mobile robot [25]. Gao *et al.* used particle filter algorithm to realize path planning of mobile robot and improve the global adaptability of robot [26]. Hsu *et al.* analyzed the signal characteristics and antenna effects of the received signal indicator, and designed a particle filter based on the current state of mobile robot to improve the positioning accuracy of the mobile robot in the wireless sensor network environment [27]. The literature [25]–[27] solve the problem of position estimation for nonlinear mobile robot system. However, the measurement data involved in estimating the position by using the particle filter algorithm is generally affected by the random errors by default, and did not consider the influence of the gross errors on the position estimation. However, there are gross errors in the actual state estimation, so we need to consider how to achieve accurate position estimation when the measurement data is affected by gross errors. Xu *et al.* proposed a two-dimensional lidar-based mobile robot pose estimation method [28]. The data points scanned by each frame of the radar were divided into clusters, and the RANSAC algorithm was used to remove the outliers in the non-complete matching clusters. This method achieved satisfactory results in the pose estimation of mobile robots in a dynamic indoor environment. Aghili *et al.* proposed integrating two real-time dynamic global positioning system units (GPS) and inertial measurement units (IMUs) in an adaptive kalman filter to compensate for errors in estimated orientation due to gyroscope drift and its paranoia, and use it for drift-free estimation of 3D vehicle pose and position [29]. Wang *et al.* proposed a mobile robot position estimation algorithm based on probability statistics and grey system theory [30]. When there were errors and outliers, the estimation accuracy was comparable to the particle filter algorithm, which was better than the extended kalman filter algorithm. When estimating a mobile robotic system, The literature [28] and [30] provided a treatment for outliers as to how to deal with gross errors in the system. literature [29] designed a drift-free estimation method for 3D vehicle attitude and position for system drift problems. However, no corresponding solution was given for how to solve the problem of two or more system errors in the system. Therefore, combining the superiority of PF in the process state estimation of nonlinear systems, this paper focuses on the different types of gross errors in the obtained measurements, such as outliers, biases and drifts when the particle filter algorithm deals with the mobile robot position estimation. The framework of this paper is divided into five parts as follows. Firstly, the

application of particle filter algorithm and the position estimation of mobile robot dynamic system are briefly described. Secondly, the principle of particle filter algorithm for position estimation is introduced. And when there are gross errors in the measurements, it is introduced how to identify and compensate these measurements in order to obtain an accurate position estimation. After that, the mobile robot system is modeled to describe the position estimation. The simulation experiment is used to verify the superiority of the proposed method in solving the problem of mobile robot position estimation with gross errors. Finally, summarize the effectiveness of the method used in this paper.

II. PRINCIPLE DESCRIPTION OF PARTICLE FILTER ALGORITHM

A typical dynamic system state space model consists of the state equation and the measurement equation as follows:

$$x_k = f(x_{k-1}, u_{k-1}) + v_{k-1} \tag{1}$$

$$y_k = h(x_k, u_k) + w_k \tag{2}$$

where $x_k \in R_x^N$ denotes the vector of states to be estimated at time step k. $y_k \in R_y^N$ is the vector of measurements at time step k. N_x is the dimension of the vector of states and N_y is the dimension of the vector of measurements. $f : R_x^N \rightarrow R_x^N$ denotes the nonlinear transition function, which defines the evolution of the vector of states as a first-order Markov process. $h : R_x^N \rightarrow R_y^N$ denotes the measurement function, which defines the relationship between the vector of states x_k and the vector of measurements y_k. u_k is the vector of the inputs. $v_{k-1} \in R_x^N$ and $w_k \in R_y^N$ are the white noise sequences for the process states and measurements.

Particle filter is based on sequential Monte Carlo approach and recursive Bayesian filter [31]. And particle filtering generally consists of two phases: the prediction phase and the update phase. Specifically, the system model (Equation 1) is used in the prediction phase to predict the prior probability density of the state, which means guessing the future state through the prior knowledge, that is $p(x_k|x_{k-1})$ During the update process, the prior probability density is corrected using the latest measurements in order to obtain the posterior probability density, which is to correct the previous guess.

First, a set of random samples is obtained from $p(x_k|x_{k-1})$,called particles $\{x_k^i, i = 1, \ldots, N\}$, and i denotes the ith particle. In the prediction phase, these particles at time k $-$ 1 are used to calculate a priori sample set at time k according to the state transition equation (3).

$$x_k^i = f(x_{k-1}^i, u_{k-1}) + v_{k-1}^i \tag{3}$$

where v_{k-1}^i is independent samples extracted from the system probability density function (PDF) with noise.

In the update phase, the weight of each particle $\{w_k^i, i = 1, \ldots, N\}$ is calculated from the measurement data y_k and the prior samples. $w_k^i = p(y_k|x_k^i)$, where $p(y_k|x_k^i)$ is likelihood probability. The weights are normalized in order to uniform distribution of the samples.Equation (4) gives the posterior distribution after the update.

$$p(x_k|y_{1:k}) \approx \sum_{i=1}^{N} w_k^i \delta(x_k - x_k^i) \tag{4}$$

where δ(x) is the Dirac function.

Since $p(x_k|y_{1:k})$ is not a regular PDF, direct sampling is not possible. Therefore, the importance sampling is introduced to obtain the joint weight of the particle group. By defining an importance density $q(x_k|y_{1:k})$, the joint weight is expressed as equation (5).

$$w_k^i \propto \frac{p(x_k^i|y_{1:k})}{q(x_k^i|y_{1:k})} \tag{5}$$

Use the state transition probability function as the suggested distribution, which means $q(x_k^i|x_{k-1}^i, y_k) = p(x_k|x_{k-1})$, then

$$w_k^i \propto w_{k-1}^i p(y_k|x_k^i) \tag{6}$$

The formula (6) is normalized to obtain the formula (7).

$$\widetilde{w_k^i} = \frac{w_k^i}{\sum_{i=1}^{N} w_k^i} \tag{7}$$

During the iterative process, due to particle degradation, the covariance of importance weights will increase, which will adversely affect the accuracy of state estimation. Therefore, the resampling is introduced. And parent particles with big weights (x_k^i) are copied as child particles, and the parent particles with small weights are discarded. Set the effective number of particles (Neff) to measure the degradation degree of the particle weights, as shown in equation (8).

$$\hat{N}eff \approx \frac{1}{\sum_{i=1}^{N} (w_k^i)^2} \tag{8}$$

After resampling, the posterior estimate of the child particles is as shown in equation (9).

$$\widetilde{p}(x_k|y_{1:k}) = \frac{1}{N} \sum_{i=1}^{N} N_k^i \delta(x_k - x_k^i) \tag{9}$$

where N_k^i denotes the number of child particles after resampling.

The state estimation vector is as shown in equation (10), and the correction measurement is calculated as shown in equation (11).

$$\hat{x_k} = \frac{1}{N} \sum_{i=1}^{N} N_k^i x_k^i \tag{10}$$

$$\hat{y_k} = h(\hat{x_k}, u_k) \tag{11}$$

The principle of the generalized particle filter algorithm is as follows:

1) Input: x_{k-1}^i; w_{k-1}^i; y_k;

2) Particle initialization: Get the particles $\{x_k^i, i = 1, \ldots, N\}$ from $p(x_k|x_{k-1})$, and set the initial weight of particles to be $w_0 = \frac{1}{N}$;

3) Calculating the likelihood probability: $p(y_k|x_k^i)$;
4) Calculating weight: $w_k^i \propto w_{k-1}^i p(y_k|x_k^i)$;
5) Weight normalization: $\widetilde{w_k^i} = \frac{w_k^i}{\sum_{i=1}^N w_k^i}$;
6) Calculating posterior estimation: $\widetilde{p}(x_k|y_{1:k}) = \frac{1}{N}\sum_{i=1}^N N_k \delta(x_k - x_k^i)$;
7) Calculating state estimation vector $\hat{x_k} = \frac{1}{N}\sum_{i=1}^N N_k^i x_k^i$ and corrected measurement $\hat{y_k} = h(\hat{x_k}, u_k)$;
8) Calculating measurement residuals $r_k = y_k - \hat{y_k}$ and testing the measurements;
9) Detecting and identifying gross errors;
10) Compensated measurement $y_k' = y_k - C_{m,k}$, update the corresponding weights: $w_k^i \propto w_{k-1}^i p(y_k'|x_k^i)$. And then resampling;
11) Updating state estimation and residuals;
12) End.

III. GROSS ERRORS TYPE DETECTION AND MEASUREMENTS COMPENSATION

Because random errors exist in any system measurements, and the existence of random errors can cause errors between the measured variables and the true values. In previous studies, it was generally assumed that the measurement data obtained from the system was only disturbed by random errors. However, in practical systems, measurement data may also be affected by non-random events, that is gross errors. And the gross errors are generally caused by single or multiple reasons, such as instrument failure, measurement equipment correction errors, sensor damage, analog-to-digital conversion errors, and process defects. It can be said that the existence of random errors reduces the accuracy of the measurement information, while gross errors introduce inaccurate information. Therefore, obtaining accurate measurement data is of great significance for the evaluation of state estimation.

A. GROSS ERRORS CLASSIFICATION

This paper studies the gross errors of the three types of outliers, biases, and drifts. figure 1 shows the measurement data with different gross errors based on the performance characteristics of these three gross errors. figure 1.(a) shows the measurements with outliers. figure 1.(b) shows the measurements with biases. figure 1.(c) shows the measurements with drifts. And the hollow dots denotes true value, yellow dots denotes measurements without gross errors, and red dots denotes measurement data with gross errors.

1) OUTLIERS

As shown in figure 1(a), the outliers have several burst peaks in the measurements. If the outliers occur in the mth measurement of the k_0 step, then its observation function can be expressed as shown in Equation (12) below:

$$\begin{cases} y_k = h(x_k, u_k) + w_k, & k \neq k_0 \\ y_k = h(x_k, u_k) + w_k + \begin{bmatrix} 0 \\ O_{m,k_0} \\ 0 \end{bmatrix}, & k = k_0 \end{cases} \tag{12}$$

where O_{m,k_0} denotes the magnitude of the mth outlier of the k_0 step.

2) BIASES

Biases are also known as residual errors. They refer to the residual deviations after thecompletion of the transition process, that is, the difference between the stable value of the controlled variable and the given value. And the values can be positive or negative, which are the important indicators of accuracy. The requirement of biases in production is limited to a small allowable range near a given value.

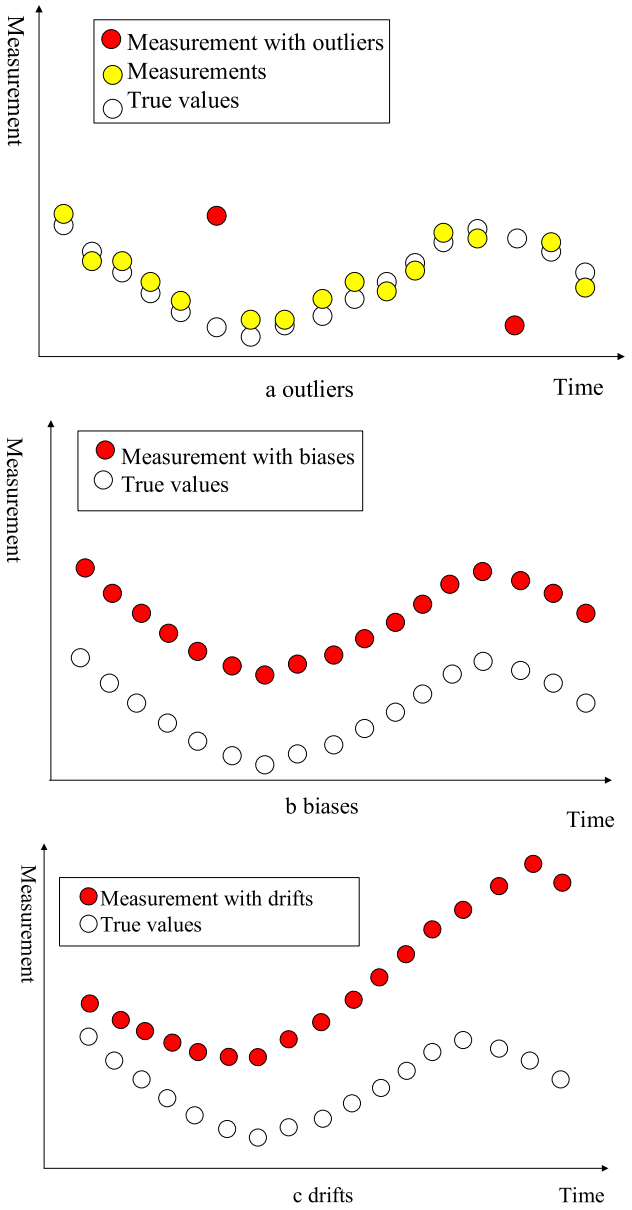

FIGURE 1. Measurements with different gross errors, (a)outliers, (b) biases, (c)drifts.

As can be seen from figure 1(b), the systematic biases are often represented by continuous and relatively stable errors on the measured device. In the case of the deviation of the

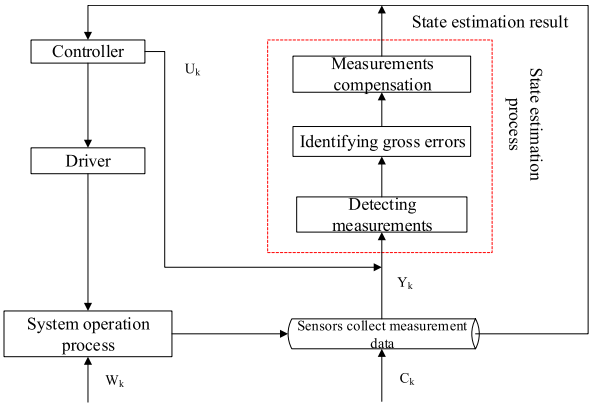

FIGURE 2. State estimation system framework based on particle filtering.

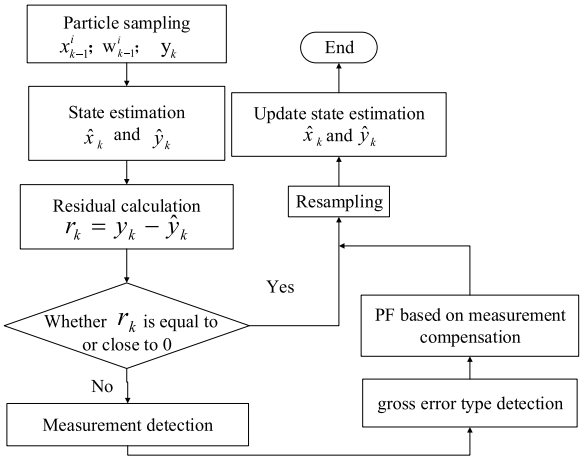

FIGURE 3. Improved particle filter algorithm based on gross error.

mth measurement, the observation function becomes:

$$y_k = h(x_k, u_k) + w_k + \begin{bmatrix} 0 \\ B_m \\ 0 \end{bmatrix} \tag{13}$$

where B_m is the biases of the mth measurement.

3) DRIFTS

Drifts reflect the ability of a measuring instrument to continuously or incrementally change its measurement characteristics over a period of time under specified conditions, maintaining its constant measurement characteristics for a certain period of time. Drifts are often caused by external factors such as pressure, temperature, humidity and unstable internal factors of the instrument's own performance. Therefore, preheating, isothermal and other measures should be taken to reduce drifts before using the measuring instrument. As can be seen from figure 1(c), if the measurement error is drift, it will be difficult to correct. Measurement errors with drifts are much more complicated than the other two types of errors. When the mth measurements drift, the measurement

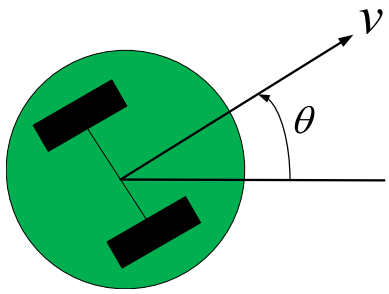

FIGURE 4. The nonlinear system description of the mobile robot.

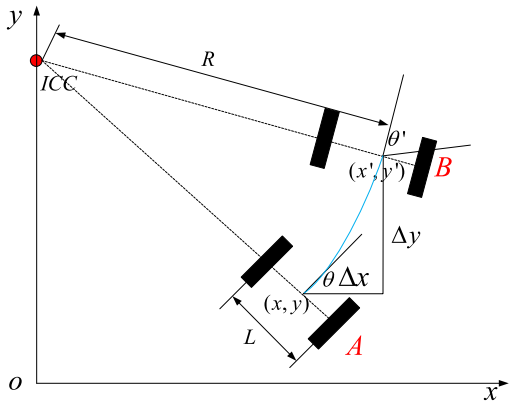

FIGURE 5. The dynamic model of mobile robot.

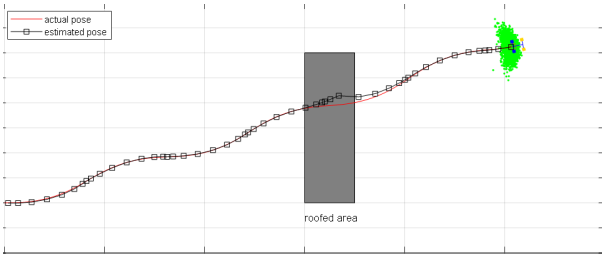

FIGURE 6. Overall operation of the mobile robot.

function becomes:

$$y_k = h(x_k, u_k) + w_k + \begin{bmatrix} 0 \\ D_m(k) \\ 0 \end{bmatrix} \tag{14}$$

where $D_m(k)$ is a function describing the drift variation of the measurement errors, which may be a linear, nonlinear or even periodic function. And it is assumed here that the function is continuous and locally linearizable.

Since gross errors have a negative impact on state estimation, they should be detected in state estimation based on particle filter in order to achieve accurate state estimation. figure 2 shows the framework of a state estimation system based on particle filtering. It consists of three parts: detecting measurements, identifying gross errors, and measurement compensation.

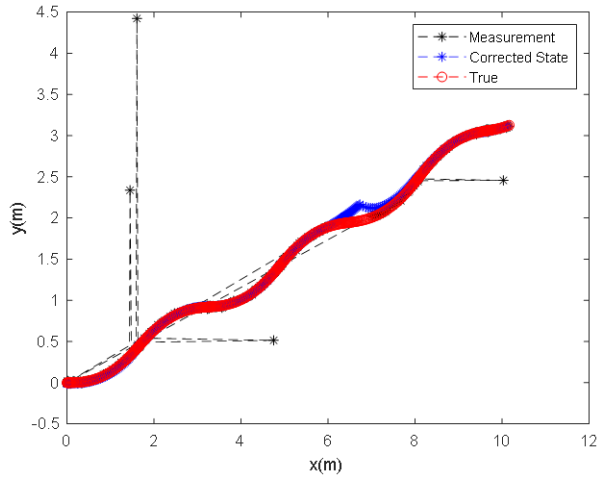

(a) Uncompensated position estimation trajectory

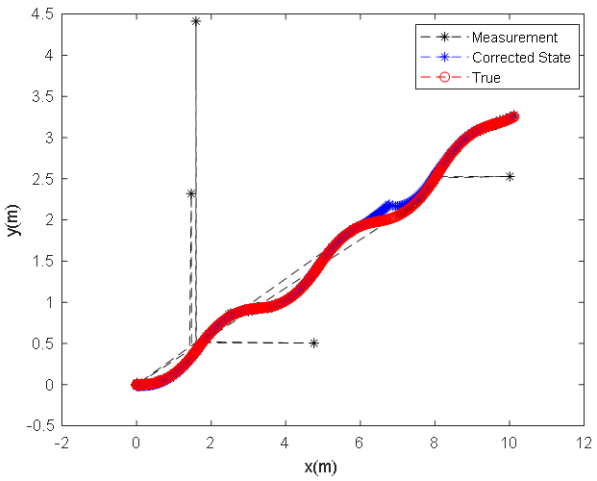

(b) Compensated position estimation trajectory

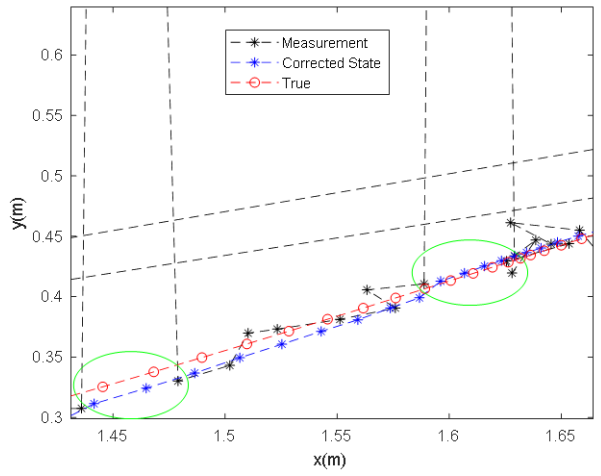

(c) Uncompensated partial enlargement

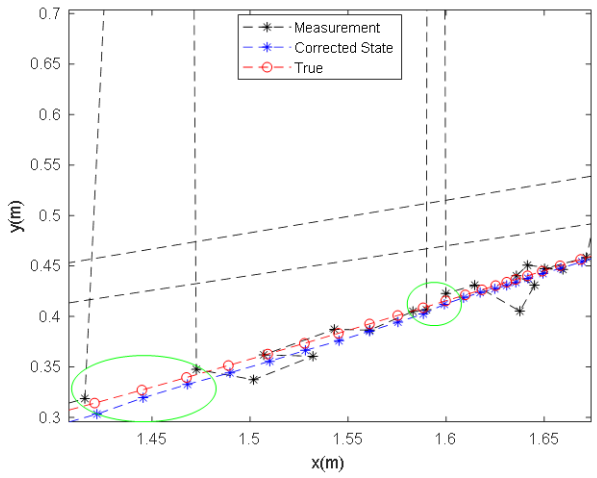

(d) Compensated partial enlargement

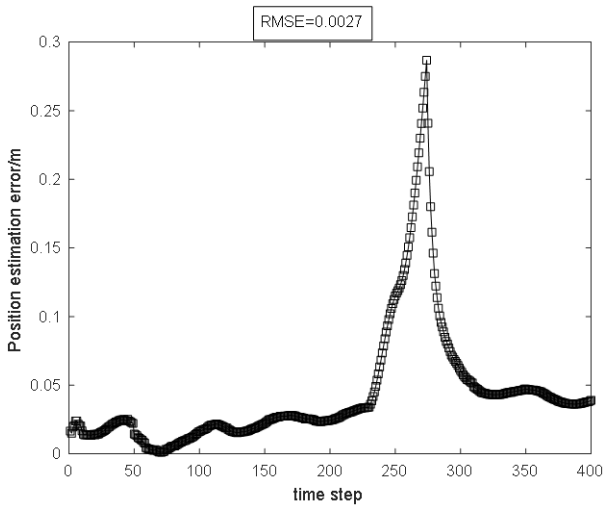

(e) Tracking error RMS of uncompensated PF

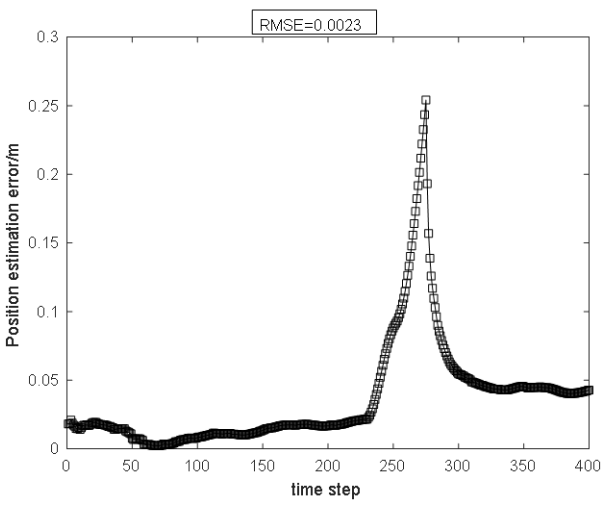

(f) Tracking error RMS of compensated PF

FIGURE 7. Position estimation in the case of outliers.

B. THE METHOD OF GROSS ERRORS DETECTION

When measurements with gross errors, the measurement function can be expressed as:

$$y_k = h(x_k, u_k) + w_k + C_k \tag{15}$$

where $C_k = [C_{1,k}, C_{2,k} \ldots, C_{N_y,k}]^T$ represents the gross error vector at time k. And $C_{m,k}$ represents the gross error information of the mth measurements at time k.

$$C_{m,k} = \begin{cases} 0 & no\ \ gross\ \ error \\ O_{m,k_0} & outlier \\ B_m & bias \\ D_m(k) & drift \end{cases} \tag{16}$$

According to the running system in figure 2 and the formula (11) of corrected measurements, it can be concluded that the residual r_k of the system can be expressed as:

$$r_k = y_k - h(\hat{x_k}, u_k) = y_k - \hat{y_k} \tag{17}$$

When there is no gross error in the measurements, the residual r_k is equal to zero or close to zero. Conversely, when the measurements with gross errors, the residual r_k will be significantly different from 0. This means that the residual should be independent of the systematic input or output, so that $r_k = w_k$ should satisfy two assumptions: (1) the expectation of w_k is $E(w_k) = 0$; (2) The covariance of w_k is known, $E(w_k w_k^T) = R$.

Tamhane and Mah used measurement test (MT) method for data correction and gross error detection in steady-state systems [32]. In this paper, MT is extended to dynamic systems for gross error detection. And the residual can be used to test for the possibility of gross errors. A statistical method of hypothesis testing is used to determine whether has gross error between the measurements and the true values. Whether $C_(m, k)$ is zero or not, the null hypothesis H_0 and the alternative hypothesis H_1 of $r_(m, k)$ are set.

$$\begin{cases} H_0 : r_{m,k} = no\ \ gross\ \ error \\ H_1 : r_{m,k} \neq no\ \ gross\ \ error \end{cases}$$

The formula used for the hypothesis test is:

$$Z_{m,k} = \frac{1}{\sqrt{R_{mm}}} |r_{m,k}| \tag{18}$$

where $Z_(m, k)$ obeys the standard Gaussian distribution $N(0, 1)$ under the null hypothesis H_0, and R_{mm} is the diagonal vector of R. When the detection statistic $y_{m,k}$ satisfies $y_{m,k} < Z_{\alpha/2}$, H_0 is accepted. Where $Z_{\alpha/2}$ is the standard Gaussian distribution of percent, and $Z_{\alpha/2}$ is not equal to zero but depends on the value of α. This hypothesis test means that when the significance level α is selected, most of the measurement errors will fall within the interval of $(1 - \alpha)$. Therefore, any measurement that falls outside the area will be considered a gross error. The probability that a gross error does not exist and is misjudged as being present is less than or equal to the prescribed significance level α.

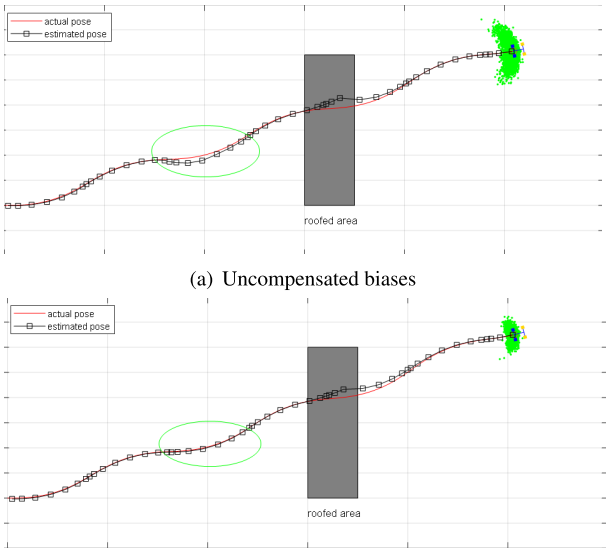

(a) Uncompensated biases

(b) Compensated biases

FIGURE 8. Position estimation in the case of outliers.

1) OUTLIERS

Since the outliers are mainly in the form of independent and accidental peaks, the outliers at a certain moment are often not associated with other moments. The detection of the outliers are performed using a distance scale based on the measured residual vector r and the response time point k. For example, if the mth measurement data contains a gross error at time k_c, then the residual point is (f_c, r_{m,k_c}). And its minimum distance $D_{\min}$ from all other measured residual points k_c', $r_{m,k_c'}$ can be expressed as:

$$D_{\min(m,k_c)} = \min(|k_c - k_c'| + |r_{m,k_c} - r_{m,k_c'}|)\ k_c \neq k_c' \tag{19}$$

Since the biases and drifts are manifested in many continuous data points, and the outliers are composed of several isolated burst peaks. So the $D_{min}$of biases and drifts are significantly lower than outliers. When there is no outlier in the measurements, all D_{min} points and $D_{min(m,k_c)}$ should satisfy the random distribution. In order to test this hypothesis, the following hypothesis in the test procedure should satisfy the Gaussian distribution.

$$\begin{cases} H_0 : (k_c, r_{m,k_c}) \neq outlier \\ H_1 : (k_c, r_{m,k}) = \ no\ \ outlier \end{cases}$$

When the testing statistic D_{min} satisfies $D_{min} < Z_(\alpha/2)$, H_0 is accepted, that is, $y_{m,k}$ is considered not to be an outlier. Conversely, when the alternative hypothesis H_1 is satisfied, $y_{m,k}$ is considered to be an outlier. And the outlier can be expressed as:

$$C_{m,k} = O_{m,k_0} = r_{m,k} \tag{20}$$

2) BIASES

The biases are the continuous and relatively stable errors on the measuring device. In this paper, the residual time series

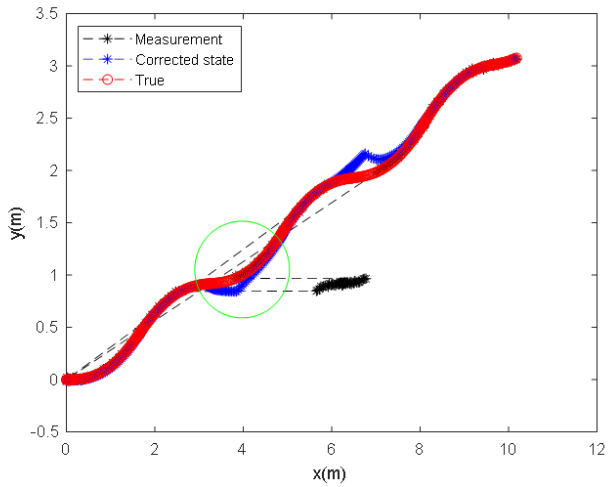

(a) Uncompensated biases

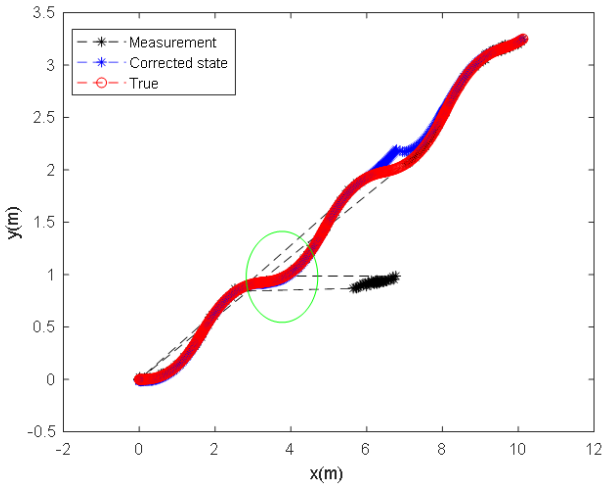

(b) Compensated biases

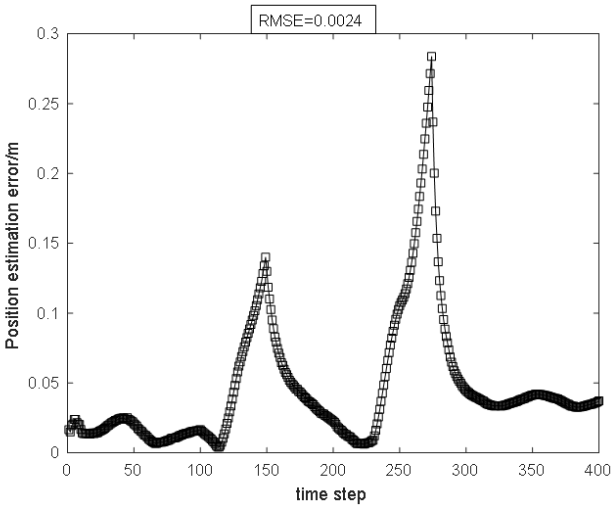

(c) Compensated biases

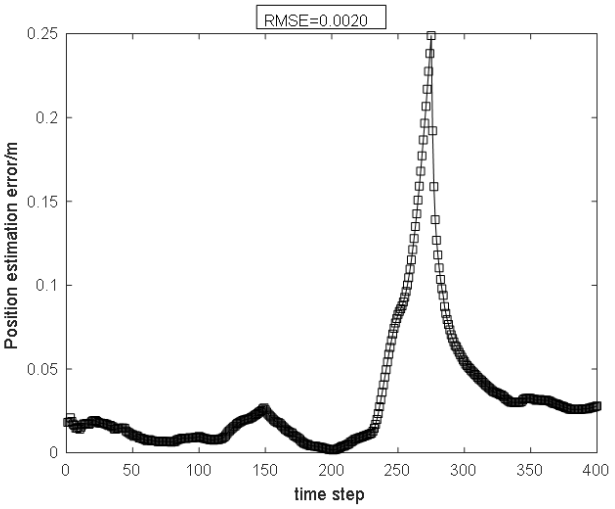

(d) Compensated biases

FIGURE 9. Position estimation in the case of outliers.

$r_{m,1}, r_{m,2}, \ldots, r_{m,k}$ of the measurement m are used to estimate the errors of measurements including biases. As shown in Equation (21) and Equation (22), the mean and variance of the data points $r_{m,k-W+1}, r_{m,k-W+2}, \ldots, r_{m,k}$ is calculated using a time window in which the span is W.

$$\bar{r}_{m,k} = \frac{1}{W}\sum_{i=1}^{W} r_{m,k} - W + i \tag{21}$$

$$S^2 = \frac{1}{W-1}\sum_{i=1}^{W}(r_{m,k-W+i} - \bar{r}_{m,k})^2 \tag{22}$$

Since the interference w_k obeys the white noise sequence and the variance S^2 obeys the F distribution, so an appropriate threshold can be selected to identify which measurements are currently most relevant to the two gross errors of biases or drifts. The variance of S^2 can be obtained by the following hypothesis test:

$$\begin{cases} H_0: & S^2 \le R_{mm} \\ H_1: & S^2 > R_{mm} \end{cases}$$

According to the characteristics of biases and drifts, the systematic biases will produce stable continuous errors, so the variance of these latest W points will be much smaller than points where the drift occurs. The one-sided hypothesis test for the statistic S^2 is obtained based on the F-distribution. When the variance S^2 is smaller than the predefined threshold ε, the data point corresponding to the mth measurement is determined to be a bias, otherwise it is classified as a drift. The size of the mth measurement with bias is estimated as follows:

$$C_{m,k} = \hat{B}_m = \bar{r}_{m,k} \tag{23}$$

3) DRIFTS

When describing the drift function $D_m(k)$, the method of a linear regression based on residuals is used to analyze the trend. And then the slope and intercept after fitting are used to estimate the variance. So the mth measurement with drift is calculated as follows:

$$C_{m,k} = D_m(k) \approx a_{m,k}k + b_{m,k} \tag{24}$$

C. GROSS ERROR COMPENSATION

The existence of gross errors can adversely affect the result of state estimation. Therefore, after detecting gross errors and determining their size, they should be eliminated to compensate for the measurements. The compensated measurements y'_k can be expressed as:

$$y'_k = y_k - C_{m,k} \tag{25}$$

Updating the corresponding weights as follows:

$$w^i_k \propto w^i_{k-1} p(y'_k | x^i_k) \tag{26}$$

The updated weights are used in resampling of particle filter, and the state variable estimate $\hat{x_k}$ and the corrected measurement $\hat{y_k}$ are derived. The measurement residual information is obtained by updating the measurements by $r_k = y_k - (\hat{y_k})$.Since $C_{m,k}$ is estimated from the measuring residual time series, the updated measurement residual can be used to improve subsequent measurements compensation.

After considering the gross errors, the principle of the improved particle filter algorithm based on gross errors is shown in figure 3.

IV. MOBILE ROBOT POSITION ESTIMATION

In this paper, the mobile robot is used as the research object, and the particle filter algorithm is used for its position estimation pro. Considering the problem that the collected measurements contain gross errors, the improved algorithm of the third chapter is used to realize the accurate position estimation of the mobile robot.

A. MODELING A MOBILE ROBOT

The nonlinear system description of the mobile robot is shown in Figure 4.

$$\begin{cases} \dot{x} = v\cos(\theta) \\ \dot{y} = v\sin(\theta) \\ \dot{\theta} = w \end{cases} \tag{27}$$

where v denotes the linear velocity of the robot, w is the steering angular velocity, and x, y and θ denote the position and posture, which can be obtained by the GPS of the mobile robot. Due to the existence of noise, there are errors in both measurement and control, that is, noise information exists in both v and w.

Put this model into the coordinate system and establish its dynamic model as shown in Figure 5.

Based on the kinematics model, a state space model of the particle filter algorithm (including state equations and measurement equations) is established. The state space model includes six state variables, which are: $x, y, \theta, v_x, v_y, v_\theta$. Where v_x and v_y represent the linear velocities of the x-axis and the y-axis, respectively. And v_θ represents the steering angular velocity, that is, $v_\theta = w$. As shown in equations (29), the state space model can be obtained by

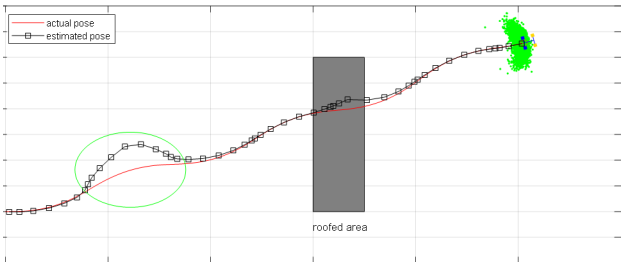

(a) Uncompensated drifts

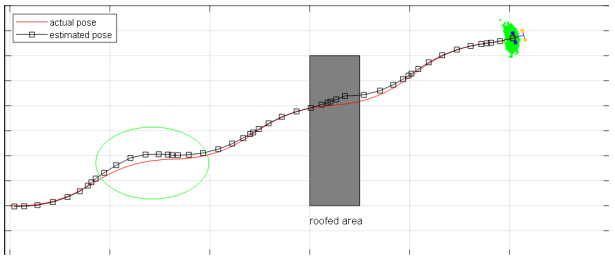

(b) Compensated drifts

FIGURE 10. Overall operation of the mobile robot.

combining equations (27), (28) and (29).

$$x_k = \begin{cases} x_1(k) \\ x_2(k) \\ x_3(k) \\ x_4(k) \\ x_5(k) \\ x_6(k) \end{cases} = \begin{cases} x_1(k-1) - (\frac{v}{w})\sin\theta(k-1) + \\ (\frac{v}{w})\sin(\theta(k-1) + w * \Delta T); \\ \\ x_2(k-1) + (\frac{v}{w})\cos\theta(k-1) - \\ (\frac{v}{w})\cos(\theta(k-1) + w * \Delta T); \\ \\ x_3(k-1) + w * \Delta T + \gamma\Delta T; \\ \\ [-(\frac{v}{w})\sin\theta(k-1) + (\frac{v}{w})\sin(\theta(k-1) \\ + w * \Delta T)]/\Delta; \\ \\ [(\frac{v}{w})\cos\theta(k-1) - (\frac{v}{w})\cos(\theta(k-1) \\ + w * \Delta T)]/\Delta T; \\ \\ w + \gamma; \end{cases} \tag{28}$$

$$y_k = h(x_k, u_k) + w_k = x_k + w_k \tag{29}$$

where $x_1(k) \sim x_6(k)$ represents the above six state variables. v and w are measured variables with random noise, and γ is random noise added to the steering angular velocity.

B. MOBILE ROBOT SIMULATION EXPERMENT

In the simulation experiment, the initial position of the mobile robot is set to move from the origin. The sampling time is 20s, the sampling interval is 0.05s, and the number of sampling particles is 5000.

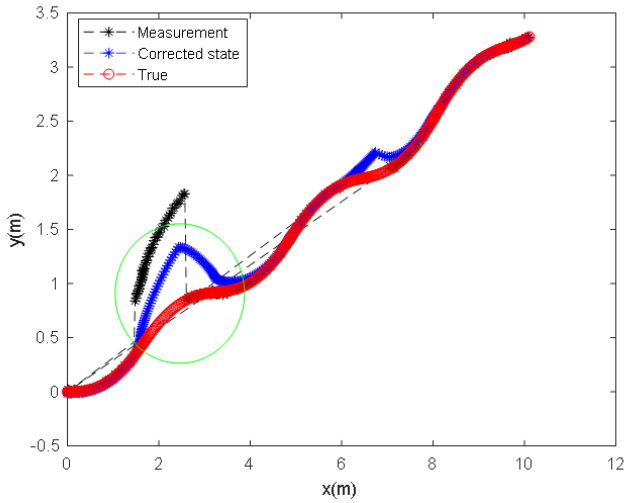

(a) Uncompensated position estimation trajectory

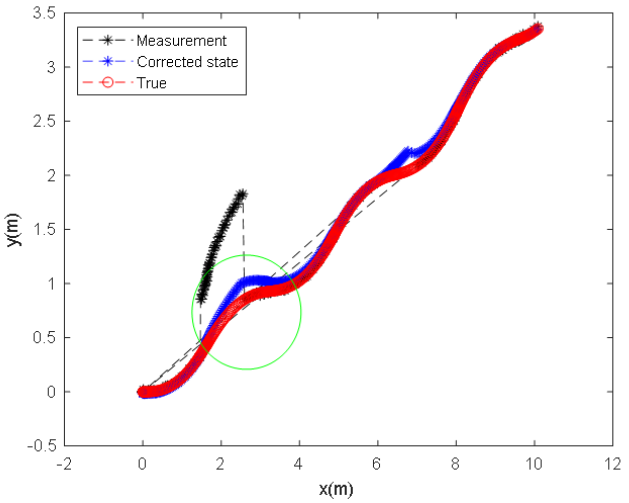

(b) Compensated position estimation trajectory

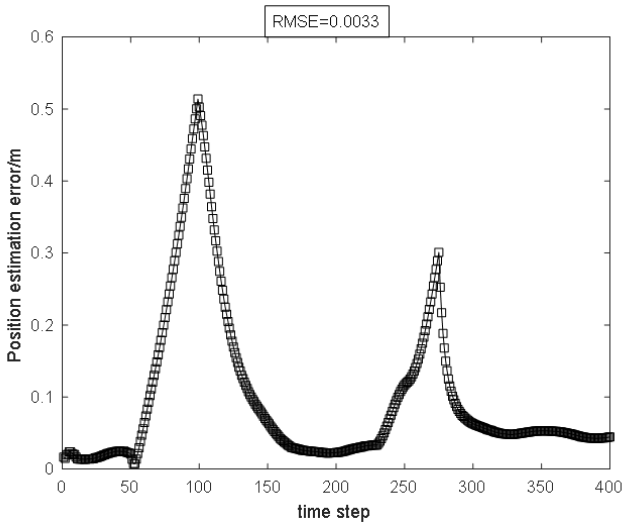

(c) Tracking error RMS of uncompensated PF

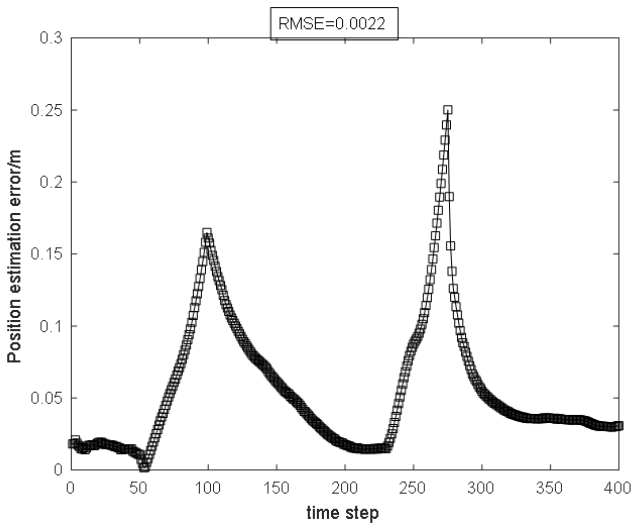

(d) Tracking error RMS of compensated PF

FIGURE 11. **Position estimation in the case of biases.**

1)Add outliers at different times and compare the accuracy of the position estimates before and after compensation. The overall operation of the mobile robot in the area is shown in Figure 6. The black part is the area blocked by the house, indicating that no measurement signal is received in this area. The red line indicates the true pose of robot, and the black square line indicates the estimated pose of the robot.

Figure 7 shows the operation of the mobile robot by adding outliers at 2.5s, 2.95s, 3.7s and 15.5s. Figure 7(a) is an uncompensated position estimation trajectory. Figure 7(b) is a compensated position estimation trajectory. figure 7(c) is a partial enlarged view of (a). figure 7(d) is a partial enlarged view of (b). Figure 7(e) shows the tracking error RMS of the PF which is not compensated after adding outliers. Figure 7(f) shows the tracking error RMS of the PF which is compensated after adding outliers. The black star-shaped dotted line denotes measurments, the blue star-shaped dotted line indicates the state corrected state values, and the red circled dotted line indicates true values. The range indicated by the ellipse is that outliers are added at 2.5s (that is, the number of iterations is 50th) and 2.95s (that is, the number of iterations is 59th).

2)Add the systematic biases at different times, and compare the accuracy of the position estimation before and after the compensation of measurements. The overall operation of the mobile robot in the area is shown in Figure 8. The black part is the area blocked by the house, indicating that no measurement signal is received in this area. The red line indicates the true pose of the robot, and

the black square line indicates the estimated pose of the robot.

Figure 9 shows the operation of the system after adding biases over a period of time. Figure 9(a) is an uncompensated position estimation trajectory. Figure 9(b) is a compensated position estimation trajectory. Figure 9(c) shows the tracking error RMS of the PF when biases are not compensated. Figure 9(d) shows the tracking error RMS of the PF when biases are compensated. The black star-shaped dotted line indicates the measurements, the blue star-shaped dotted line indicates the corrected state values, and the red circled dotted line indicates the true values.

3)The drift is added to the mobile robot system. And compare the accuracy of the position estimation before and after the compensation of measurements. The overall operation of the mobile robot in the area is shown in Figure 10. The black part is the area blocked by the house, indicating that no measurement signal is received in this area. The red line indicates the true pose of the robot, and the black square line indicates the estimated pose of the robot.

Figure 11 shows the operation of the system after adding drifts over a period of time. Figure 11(a) is an uncompensated position estimation trajectory. Figure 11(b) is a compensated position estimation trajectory. Figure 11(c) shows the tracking error RMS of the PF when drifts are not compensated. Figure 11(d) shows the tracking error RMS of the PF when drifts are compensated.

The black star-shaped dotted line indicates the measurements, the blue star-shaped dotted line indicates the corrected state values, and the red circled dotted line indicates the true values.

It can be seen from the root mean square error of three gross errors that using the improved particle filter algorithm to deal with the gross errors will make the position estimation of the mobile robot more accurate.

V. CONCLUSION

The improved particle filter algorithm is used to identify and compensate for the gross errors in measurements. And the influence of gross errors on the accuracy of the position estimation in the dynamic state estimation of the mobile robot is solved. In the simulation experiment, three kinds of gross errors are set in the case of compensation and uncompensation. The magnitude of the root mean square error of the mobile robot's position estimation is compared, which shows that the improved particle filter algorithm has superiority in processing the mobile robot system. This proves the effectiveness of the proposed method in estimating the position of mobile robots.

REFERENCES

[1] X. Wang, L. T. Yang, X. Xie, J. Jin, and M. J. Deen, "A cloud-edge computing framework for cyber-physical-social services," *IEEE Commun. Mag.*, vol. 55, no. 11, pp. 80–85, Nov. 2017.

[2] X. Wang, L. T. Yang, L. Kuang, X. Liu, Q. Zhang, and M. J. Deen, "A tensor-based big-data-driven routing recommendation approach for heterogeneous networks," *IEEE Netw.*, vol. 33, no. 1, pp. 64–69, Jan. 2019.

[3] X. Deng, M. Xu, L. T. Yang, M. Lin, L. Yi, and M. Wang, "Energy balanced dispatch of mobile edge nodes for confident information coverage hole repairing in IoT," *IEEE Internet Things J.*, vol. 6, no. 3, pp. 4782–4790, Jun. 2019.

[4] X. Deng, L. T. Yang, L. Yi, M. Wang, and Z. Zhu, "Detecting confident information coverage holes in industrial Internet of Things: An energy-efficient perspective," *IEEE Commun. Mag.*, vol. 56, no. 9, pp. 68–73, Sep. 2018.

[5] B. Wang, Q. Yang, and X. Deng, "Energy management for cost minimization in green heterogeneous networks," *Future Gener. Comput. Syst.*, vol. 105, pp. 973–984, Apr. 2020.

[6] L. Ren, Y. Laili, X. Li, and X. Wang, "Coding-based large-scale task assignment for industrial edge intelligence," *IEEE Trans. Netw. Sci. Eng.*, early access, Sep. 18, 2019, doi: 10.1109/TNSE.2019.2942042.

[7] X. Wang, L. T. Yang, H. Li, M. Lin, J. Han, and B. O. Apduhan, "NQA: A nested anti-collision algorithm for RFID systems," *ACM Trans. Embedded Comput. Syst.*, vol. 18, no. 4, pp. 1–21, Jul. 2019, doi: 10.1145/3330139.

[8] J. Cui, L. Ren, X. Wang, and L. Zhang, "Pairwise comparison learning based bearing health quantitative modeling and its application in service life prediction," *Future Gener. Comput. Syst.*, vol. 97, pp. 578–586, Aug. 2019.

[9] X. Deng, Y. Jiang, L. T. Yang, M. Lin, L. Yi, and M. Wang, "Data fusion based coverage optimization in heterogeneous sensor networks: A survey," *Inf. Fusion*, vol. 52, pp. 90–105, Dec. 2019.

[10] M. Wang, X. Wang, L. T. Yang, X. Deng, and L. Yi, "Multi-sensor fusion based intelligent sensor relocation for health and safety monitoring in BSNs," *Inf. Fusion*, vol. 54, pp. 61–71, Feb. 2020.

[11] J. Xiao, "Improvement of particle filter algorithm and its application research," East China Jiaotong Univ., Nanchang, China, 2017.

[12] N. Zhao, "Research and improvement of particle filter algorithm," Harbin Eng. Univ., Harbin, China, 2009.

[13] Y. F. Han, "Research on particle filtering and improved algorithm in multi-carrier CDMA system," Harbin Eng. Univ., Harbin, China, 2011.

[14] K. Zhang, Y. Zhu, S. Maharjan, and Y. Zhang, "Edge intelligence and blockchain empowered 5G beyond for the industrial Internet of Things," *IEEE Netw.*, vol. 33, no. 5, pp. 12–19, Sep. 2019.

[15] Z. Zhu, Z. Meng, Z. Zhang, J. Chen, and Y. Dai, "Robust particle filter for state estimation using measurements with different types of gross errors," *ISA Trans.*, vol. 69, pp. 281–295, Jul. 2017.

[16] M. Vaghefi, K. Mahmoodi, and M. Akbari, "Detection of outlier in 3D flow velocity collection in an open-channel bend using various data mining techniques," *Iranian J. Sci. Technol., Trans. Civil Eng.*, vol. 43, no. 2, pp. 197–214, Jun. 2019.

[17] F. P. Xie and W. G. Jiang, "Tracking biases analysis and elimination of concentrating photovoltaic biaxial daily tracking system under time-controlled algorithm," *Renew. Energy*, vol. 35, no. 10, pp. 1471–1478, 2017.

[18] J.-S. Wang and G.-H. Yang, "Data-driven compensation method for sensor drift faults in digital PID systems with unknown dynamics," *J. Process Control*, vol. 65, pp. 15–33, May 2018.

[19] Z. Zhang and J. Chen, "Simultaneous data reconciliation and gross error detection for dynamic systems using particle filter and measurement test," *Comput. Chem. Eng.*, vol. 69, pp. 66–74, Oct. 2014.

[20] C. S. Maiz, E. M. Molanes-Lopez, J. Miguez, and P. M. Djuric, "A particle filtering scheme for processing time series corrupted by outliers," *IEEE Trans. Signal Process.*, vol. 60, no. 9, pp. 4611–4627, Sep. 2012.

[21] S. M. Malagon-Soldara, E. D. Avalos-Rivera, and E. A. Rivas-Araiza, "Localization for indoor applications with a cheap sonar by particle filter estimation," in *Proc. 8th Euro Amer. Conf. Telematics Inf. Syst. (EATIS)*, Apr. 2016, pp. 1–8.

[22] J. X. Shou, Z. M. Zhang, and Y. Q. Su, "Design and implementation of indoor mobile robot positioning and navigation system based on ROS and Lidar," *Machinery Electron.*, vol. 36, no. 11, pp. 76–80, 2018.

[23] M. Alatise and G. Hancke, "Pose estimation of a mobile robot based on fusion of IMU data and vision data using an extended Kalman filter," *Sensors*, vol. 17, no. 10, p. 2164, 2017.

[24] Y. Dobrev, S. Flores, and M. Vossiek, "Multi-modal sensor fusion for indoor mobile robot pose estimation," in *Proc. IEEE/ION Position, Location Navigat. Symp. (PLANS)*, Apr. 2016, pp. 553–556.
[25] A. Canedo-Rodriguez, J. Rodriguez, V. Alvarez-Santos, R. Iglesias, and C. Regueiro, "Mobile robot positioning with 433-MHz wireless motes with varying transmission powers and a particle filter," *Sensors*, vol. 15, no. 5, pp. 10194–10220, 2015.
[26] Y. Gao, S. Sun, D. Hu, and L. Wang, "An online path planning approach of mobile robot based on particle filter," *Ind. Robot, Int. J.*, vol. 40, no. 4, pp. 305–319, Jun. 2013.
[27] C.-C. Hsu, S.-S. Yeh, and P.-L. Hsu, "Particle filter design for mobile robot localization based on received signal strength indicator," *Trans. Inst. Meas. Control*, vol. 38, no. 11, pp. 1311–1319, Nov. 2016.
[28] Y. Xu, C. Zhang, and W. Bao, "A robust pose estimation algorithm for mobile robot based on clusters," in *Proc. Int. Conf. Intell. Robot. Appl.*, vol. 5314. New York, NY, USA: Springer-Verlag, 2008, pp. 1003–1010.
[29] F. Aghili and A. Salerno, "Driftless 3-D attitude determination and positioning of mobile robots by integration of IMU with two RTK GPSs," *IEEE/ASME Trans. Mechatronics*, vol. 18, no. 1, pp. 21–31, Feb. 2013.
[30] P. Wang, Q.-B. Zhang, and Z.-H. Chen, "A grey probability measure set based mobile robot position estimation algorithm," *Int. J. Control, Autom. Syst.*, vol. 13, no. 4, pp. 978–985, Aug. 2015.
[31] D. C. Lv, J. T. Fan, and G. W. Han, "Overview of particle filtering," *Astronomical Res. Technol.*, vol. 10, no. 4, pp. 397–409, 2013
[32] A. C. Tamhane and R. S. H. Mah, "Data reconciliation and gross error detection in chemical process networks," *Technometrics*, vol. 27, no. 4, pp. 409–422, Nov. 1985.